UNIVERSITAT ROVIRA i VIRGILI

PERFORMANCE OF A SINGLE-EFFECT HOT WATER-FIRED LIBR/WATER ABSORPTION CHILLER INSTALLED IN THE UNIVERSITY OF CORDOBA. FIRST RESULTS.

JAVIER GONZÁLEZ SOLÍS

MASTER THESIS

2025

Javier González Solís

Performance of a single-effect hot water-fired LiBr/water absorption chiller installed in the University of Cordoba. First results.

MASTER'S THESIS

Supervised by

Alberto Coronas

Manuel Ruiz de Adana

Master's Degree

Energy Conversion Systems and Technologies

UNIVERSITAT
ROVIRA i VIRGILI

Tarragona, June 2025

We STATE that the present master thesis, entitled "Performance of a single-effect hot water-fired LiBr/Water absorption chiller installed in the University of Cordoba. First results" by Javier González Solís, has been carried out under our supervision.

June 23, 2025

Alberto Coronas

Manuel Ruiz de Adana

Acknowledgements

I want to thank and acknowledge Prof. Alberto Coronas for his support and help during the completion of this thesis. I am grateful for his advice and the closeness he has shown me throughout the master's degree.

I would also like to thank Prof. Manuel Ruíz de Arana for providing me with information about the demonstration plant in Córdoba.

Finally, I would also like to thank the company Carrier for the technical information they have provided, sharing details about the absorption chiller.

INDEX

1- INTRODUCTION

1.1. Background

In the current context of the energy transition and the fight against climate change, the need to reduce fossil fuel consumption and greenhouse gas emissions has driven the development of new strategies for generating, distributing, and efficiently using energy. One of the sectors with the most tremendous potential for improvement is the space heating and cooling in buildings, which account for a significant portion of total energy consumption in urban environments.

The space heating and cooling of buildings accounts for 50% of the total EU energy consumption. A large portion of this energy (70%) is currently generated from fossil fuels (coal, natural gas, and oil). By switching to fossil-free energy, this sector would bring us one step closer to climate neutrality, improve air quality in European cities, and enhance the quality of life for our citizens [1] .

District energy is a proven solution for delivering heating, hot water, and cooling services through a network of insulated pipes from a central point of generation to end-users [2] . WEDISTRICT is a European project that aims to demonstrate the reliability of renewable district heating and cooling (DHC) systems, through the integration of various renewable energy sources (solar energy, biomass, geothermal energy and waste heat), advanced thermal storage technologies to redistribute heat to buildings as needed, and innovative technologies to increase the operational efficiency of the systems. With this goal, three demonstration projects in three different European cities (Córdoba, Bucharest, and Luleå) have been selected to integrate fossil-free WEDISTRICT technologies [3] .The demonstration cases will present the best practices that can be replicated across different climate zones and building types, transforming the heating and cooling sector. Each demonstration case will be based on the integration of two or more renewable energy-based technologies, building on local resources and innovative technologies [1] .

Spain is one of the most attractive European countries for implementing solar energy technologies due to its high solar insolation. Annually, the direct normal irradiation is approximately 2 MWh/m², making concentrated solar technology a promising solution for meeting the heating demand of buildings, as well as the cooling demand through thermally activated chillers [4] .

In the Wedistrict demo project of Córdoba, several renewable technologies were implemented, including three different solar thermal technologies, a biomass boiler, and solar cooling connected to a heating and cooling network. This network has two thermal substations that cover the heating and cooling demands of the Da Vinci building and the Monte Cronos sports area. Figure 1.1 shows an overview of the Córdoba demonstration buildings.

Figure 1.1. Overview of the Córdoba demo site buildings.

As mentioned above, various technologies have been planned to be installed for the Córdoba demo site [3] [4] :

- Three types of concentration solar collectors: Parabolic Trough Collector (PTC), Linear Fresnel Collector, WeSSun (Tracking Concentrator with Fixed Tilt Collector).
- Two technologies to produce cooling from renewable energy sources: Renewable Air-Cooling Unit (RACU), Absorption Chiller.
- One thermal energy storage tank.
- Two high-efficiency, low-emission biomass boilers.

The solar technologies of parabolic trough collectors and Fresnel collectors are installed in the north of the demonstration plant, with their axes oriented East-West. On the other hand, the plate solar collectors with reflectors are installed to the south, aligned along the east-west axis. In both cases, the thermal fluid used in the collectors is water.

The heat produced by these solar thermal collectors is stored in a 50 m^3 water storage tank, which increases solar gain and makes periods of solar energy production more compatible with building demand.

Furthermore, the facility has a system for producing thermal energy from biomass. This system consists of two 500 kW boilers, equipped with an electrofilter and a polyfuel supply system.

The production of cooling is carried out by a commercial absorption chiller. The heat required by the chiller is generated by the solar thermal collectors field. In case there is not enough heat production, the biomass boilers can complete the heating required by the absorption chiller. Additionally, a renewable air-cooling unit has been implemented to provide air conditioning service to a classroom in the Da Vinci building.

The demo plant operation is designed to maximise the renewable production of cooling and heating from renewable sources, replacing as much as possible the consumption of non-renewable generating equipment in the buildings supplied. The Da Vinci building is divided into three zones. In each zone, it utilises two heat pumps to provide temperatures of up to 45/40 ºC for heating in winter and temperatures of up to 7/12 ºC for cooling in summer. Heat pumps supply hot or chilled water to the hydraulic circuit that feeds the building's terminal units, of the fan coil type. The Monte Cronos sports stadium features a gas oil boiler to generate hot water at 65 °C for the domestic hot water (DHW) of the changing rooms. The renewable energy plant will provide energy to these two buildings through a two-pipe district network consisting of pre-insulated pipes, which connect the generation plant to exchange substations in each building, where thermal energy is delivered [3] .

Regarding the distribution temperatures, the system operates under two modes:

- Cooling mode (summer mode). The absorption chiller requires hot water at temperatures between 95 and 80 ºC to ensure operation, so the main collector would typically operate at these temperatures. The distribution to the Da Vinci building is of the chilled water generated in this absorption machine at a minimum of 7/12 ºC.
- Heating mode (winter mode). The Da Vinci building requires heating at 45/40 ºC, although demand at higher temperatures (95/80 ºC) persists for the distribution of DHW in the changing rooms of Monte Cronos.

1.2. Methodology

This master's thesis focuses on the study of the performance of the commercial absorption chiller installed at the Córdoba demo site, specifically during the summer operation mode, also known as cooling mode. Therefore, the technologies explained in this report are those related to the driving heat provided to the absorption chiller: the solar thermal collectors, the water storage tank, the biomass boilers and, of course, the absorption chiller.

The commercial absorption chiller used is a single-effect hot water-fired LiBr/water absorption chiller provided by Carrier and installed in the demonstration plant at the University of Córdoba.

The chiller was commissioned by Carrier at the end of the project (September and October 2024) and is not yet operational. Therefore, in this master's thesis, the commissioning results of the machine's performance are used to model and analyse the performance. For this purpose, the available experimental data and technical information on the chiller are compiled from the tests conducted by Carrier during commissioning.

1.3. Objectives

The main objective of this thesis is to study the performance of the Carrier absorption chiller, calculating performance values and indicators such as heat rates exchanged in the main components, thermal COP and exergy COP. To fulfil this objective, the machine is described, and the input data collected in the tests carried out by Carrier are identified.

It also aims to describe the installation and technologies used at the Córdoba demonstration site to produce renewable cooling for the absorption chiller.

1.4. Methodological approach

The performance is obtained by modelling the thermodynamic absorption refrigeration cycle and heat transfer in the main thermal components, based on the temperature values measured and recorded by the machine's management data and control system, and validated using data provided by the demo instrumentation installed in the external water heating system. The model can be used to determine the performance under other operational conditions.

2- DESCRIPTION OF THE CÓRDOBA DEMONSTRATION TECHNOLOGIES

2.1. Solar Thermal Collector Technologies

Solar thermal collectors are a specialised type of heat exchanger that converts solar radiation into heat. In solar collectors, the energy transfer relies entirely on radiation heat transfer over a vast distance. The heat flux of incident solar radiation under optimal conditions is approximately 1100 W/m^2 without optical concentration. However, some solar collector technologies involve optical concentration to increase the temperature potential.

Solar thermal collectors are typically categorised into two types: stationary and tracking solar collectors. Flat-plate collectors and vacuum tube collectors (also known as evacuated tube collectors) are stationary solar collectors.

Tracking solar collectors, which are the focus of this technology assessment, can further be divided into linear and point focus solar collectors. Parabolic troughs and Fresnel collectors are examples of linear focus solar collectors, while tower and parabolic collectors are examples of point focus solar collectors.

The Seenso company designed and constructed a new low-concentration solar collector, titled the tracking concentrator with fixed tilt solar thermal collector, which represents a hybrid between the two concepts [5] .

2.1.1. WeSSun Solar Collectors

WeSSun consists of a non-focusing cylindrical concentrator that uses movable flat mirrors rotating on an axis parallel to the cylinder's axis. WeSSun has low solar concentration levels (typically C = opening area/absorbent area < 2), and it is specially designed to be coupled to evacuated tube collectors (ETC) or flat-plate solar collectors, allowing them to be used in applications requiring heat at temperatures close to 150°C with reasonable yields. The main characteristic of the device is that the concentrating flat mirrors follow the sun and redistribute the radiation available in the aperture homogenously over the absorber.

WeSSun increases the efficiency associated with concentration at a reasonable cost, and it does not experience problems regarding the stagnation temperature. As the concentrator mirrors are movable, they can be used as shading elements, thus blocking solar radiation and avoiding high stagnation temperatures when necessary. This shading position also has the advantage of minimising soiling during nighttime and non-operational periods of the plant. Furthermore, it

reduces wind and snow loads when required. The device can turn the mirrors to block the solar radiation or to protect the concentrator against high winds.

Three types of WeSSun technology have been designed at the University of Córdoba. The first concentrator is oriented along the east-west axis and laterally tilted 30º towards the equator, using large extruded polystyrene blocks as support. Another characteristic of this system is that it features two types of solar collectors: 7 Linuo XL1921 ETCs and 15 Delpaso Solar Top 3000 flat-plate collectors, which offer better performance. The surface steel density (mass of steel per unit aperture area) of this WeSSun is above 20 kg/m^2 aperture, which is much higher than the recommended value for an economically competitive concentrator. Figure 2.1 shows this concentrator with the windows open.

Figure 2.1. Concentrator Wessun placed in the Córdoba demo site.

The other two WeSSuns have an easier installation, as well as a lower steel density in the structure, at 7.1 kg/m^2. This design features a top mirror, which significantly enhances concentrator performance. These concentrators use 2-meter mirrored aluminium sheets bonded to polycarbonate sheets as a mirror and a linear actuator for the solar tracking of the top mirror. These two WeSSuns have five Delpaso Solar Top 3000 flat-plate collectors each. Figure 2.2 illustrates the 3D design of these concentrators.

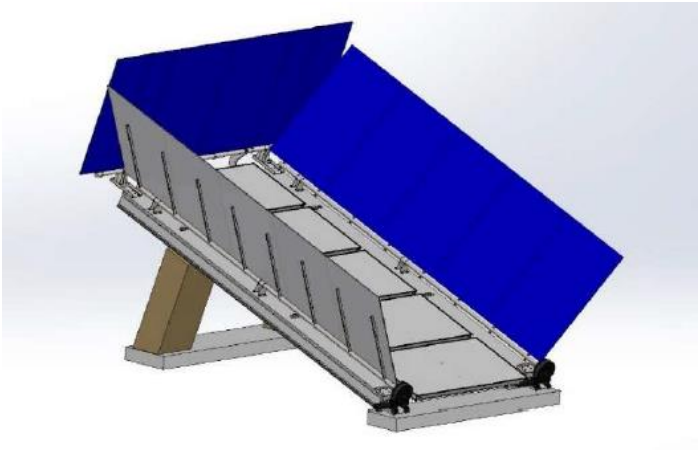

Figure 2.2. Design of the second WeSSun concentrator.

The total surface area of this solar technology is 119.55 m^2, of which 41.1 m^2 corresponds to the surface of flat collectors, 31.2 m^2 to the surface of vacuum tubes, and the rest to the surface of inclined mirrors (with tracking). The thermal power generated by WeSSun technology is 85 kWt under nominal conditions [3] .

2.1.2. Parabolic Trough Collectors

Parabolic trough collectors (PTCs) are a linear concentrating technology that consists of parabolic trough-shaped mirrors (collectors) that focus the solar radiation along a heat receiver tube (absorber) filled with a heat transfer fluid (water). The mirrors and the receiver tubes are supported by a structure made of galvanised construction steel. The main structural components are piles, tubes, and mirrors supporting rails [3] .

PTCs feature a special glass vacuum tube, guaranteeing lower heat losses and providing stable energy production even at moderate temperatures, as the receiver pipe has very low heat loss. The parabolic trough utilises a sun-tracking technology, where a computer calculates and calibrates the troughs to the required position to receive optimal radiation throughout the day [5] .

Within the context of the WeDistrict project, the aim has been to enhance the PTC technology, improving its cost competitiveness, reliability, and reducing its environmental impact. To this end, the following technological innovations have been introduced: a new wireless control and power supply system, new structural solutions, and enhanced control and monitoring software [3] .The wireless power supply and control system allows the elimination of cables between the central control panel, the panels and the necessary cable trenches. Additionally, the power

supply for the solar tracking system comes from a separate photovoltaic module and a lithium-ion battery system [6] . Figure 2.3 illustrates the PTC developed by Soltigua.

Figure 2.3. Parabolic trough collector.

The total surface area of this solar technology is 328 m^2 (82 m^2 for each parabolic trough module). The thermal power generated by PTC technology is 184 kWt under nominal conditions [3] .

2.1.3 Lineal Fresnel Collectors

Linear Fresnel collectors (LFCs) are a linear concentrating technology that consists of multiple lines of mirrors, concentrating solar radiation along a heat receiver tube (absorber). The mirrors and receiver tubes are supported by a structure made of galvanised construction steel [3] .

In Fresnel systems, mirrors concentrate the sun's rays onto elevated linear receivers that are not directly connected to them but are located several metres above the primary mirror field. The long-narrow mirror strips are pivot-mounted, allowing each to be oriented at a chosen angle, which focuses sunlight onto the receiver throughout the day [5] .

As for the PTCs, lineal Fresnel collectors also feature the same type of improvements: a new wireless control and power supply system, new structural solutions, and enhanced control and monitoring software. Figure 2.4 shows the Fresnel collectors developed by Soltigua.

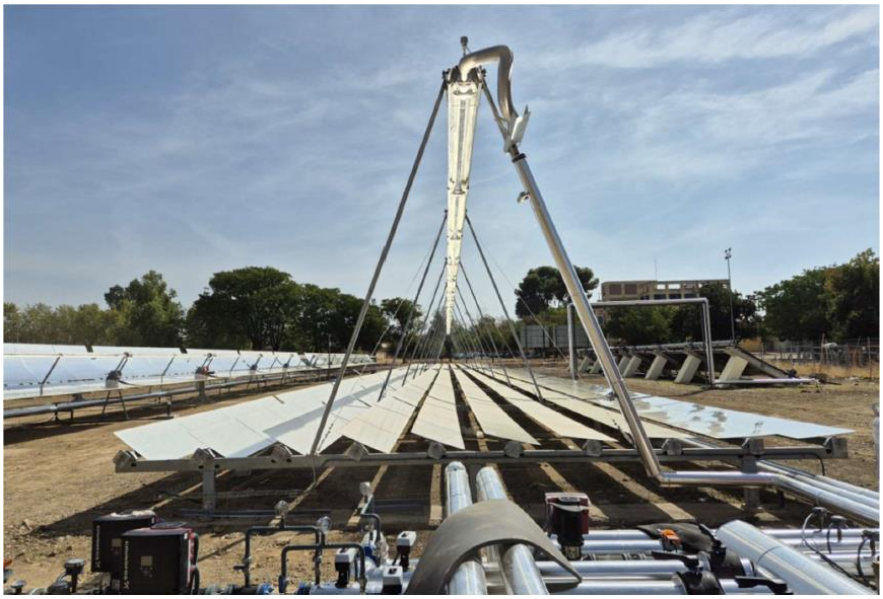

Figure 2.4. Lineal Fresnel collectors.

The total surface area of this solar technology is 445.55 m^2. The thermal power generated by Fresnel technology is 240 kWt under nominal conditions [3] .

2.2. Thermal Energy Storage Tank

Heat storage is a key component in any energy system where the energy generation is not able to follow the demand. Limitations on the management of intermittent energy sources, such as solar energy, imply the need for storage capability.

Sensible heat storage, which is the focus of WeDistrict, is a type of storage technology in which thermal energy is stored during changes in the temperature of a heat storage medium. In such systems, there are two distinct temperatures due to the density difference: the hot fluid located at the top of the tank and the cold fluid at the bottom. The intermediate zone is called the thermocline region and is characterised by a strong temperature gradient.

During charging, the hot fluid is supplied to the upper part of the storage, while the cold fluid is extracted from the bottom. The opposite occurs during discharge, the hot fluid is extracted from the upper part, while the cold fluid is supplied to the bottom. Thus, the temperature increases during charging and decreases during discharging.

Hot water tanks are sensible heat storage devices consisting of insulated steel vessels that use water as the heat storage medium. A tank with optimised volume, shape, and insulation can store hot water up to <100ºC for daily cycles (when using water as a storage medium at temperatures above 100°C, the storage system needs to be pressurised to avoid vaporisation).

These tanks can be used in combination with inflexible heat generation units, such as solar thermal collectors, to collect excess heat during periods with high availability and low demand.

At the UCO plant, solar collector technologies, which produce energy at around 95 ºC, are connected to a water storage tank. In this case, the temperature difference during the operation of the water storage is in the order of $\Delta T = 30$ °C. For example, although the maximum temperature is 100 °C, the average temperature of the tank could be 82.5 °C (between 65 °C and 95 °C).

The tank stores the thermal energy produced by the solar collectors, which supplies energy to satisfy the demand for cooling. Therefore, the total charge capacity is limited by the power of the solar collectors. The discharge rate is defined from the expected hot water demand, considering the contribution of biomass boilers. The final storage capacity of the tank is defined by optimisation between solar generation and demand, which will determine its volume. The volume of the water storage tank is 50 m^3 [5] .

2.3. Low-Emissions Biomass Boiler

Biomass boilers convert biomass, via combustion, into thermal energy in the form of either liquid water or steam. This combustion is one of the technologies capable of reducing CO_2 emissions into the atmosphere. The biomass is typically composed of wood chips, wood pellets, or straw [5] .

The two high-temperature, low-emissions biomass boilers developed by CER and TERMOSUN and implemented at the UCO demo site are designed to optimise combustion efficiency and emissions control. The biomass fuels used are pine wood chips, primarily for non-industrial purposes.

The boiler features an advanced combustion chamber with dual-zone functionality, allowing for improved thermal performance and reduced emissions. The system includes an automatic ignition mechanism with hot air blowers and a comprehensive ash centralisation system for easy maintenance. The vertical heat exchangers are equipped with an integrated cleaning system, further enhancing operational efficiency. Additionally, the automatic control system ensures precise regulation of both combustion and smoke output.

It combines new geometry furnaces and methods to reduce NOx and PM emissions even below those of natural gas combustion. The electrofilters remove fine particulate matter, such as ash and dust, from the exhaust gases produced during the combustion of biomass. This process

helps reduce air pollution and improve the overall efficiency of the biomass boiler system. The boilers, along with hydraulic and electric installations, are containerised into a pine wood lining. Figure 2.5 shows one of the biomass boilers installed at the UCO [3] .

Figure 2.5. Biomass boiler installed in the Córdoba demo site.

The total heat capacity of the two units is 1 MW, with an efficiency of 92.5% (related to the LHV, which has a minimum of 3000 kcal/kg) at full load and 94% at 20% load. The auxiliary electric energy consumption is expected to be 1% of the total heat output. The supply temperature of water to the boiler is 95 °C, with a maximum outlet temperature of 130 °C [5] .

3- ABSORPTION CHILLER

Absorption cooling cycles, such as the mechanical vapour compression refrigeration cycle, utilise the latent heat of evaporation of a refrigerant to remove heat from the entering chilled water. Currently, vapour compression refrigeration systems use synthetic refrigerants and a compressor to transport the refrigerant vapour to be condensed in the condenser. The LiBr absorption cycle, however, uses water as the refrigerant and an absorbent lithium bromide (LiBr) solution to absorb the vaporised refrigerant [7] .

3.1. Overview of LiBr/Water Absorption Chiller

The basic single-effect LiBr/water absorption chiller consists of four components that exchange energy with the surroundings (desorber, condenser, evaporator, and absorber), one internal heat exchanger, two flow restrictors (termed valves), and a pump. Below, in Figure 3.1, a block diagram of a single-effect absorption cycle is provided, represented in the LiBr/water pressure-temperature-concentration (PTX) diagram of the LiBr/water mixture.

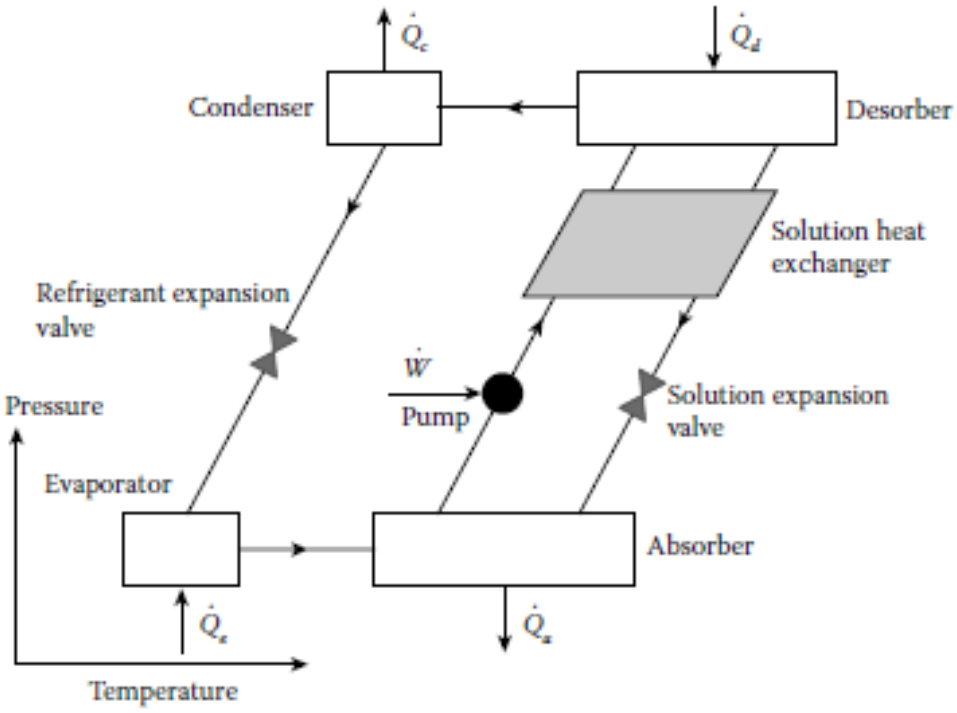

Figure 3.1. Single-effect absorption cycle schematic in the PTX diagram.

The LiBr aqueous solution circulates in the "solution circuit" connecting the desorber and absorber. The solution is pumped from the low-pressure absorber to the high-pressure desorber. As a first approximation, the entire machine can be considered to operate between two pressure levels. The solution is pumped into the desorber, where an external source supplies the driving heat with a sufficiently high temperature. For a typical single-effect aqueous lithium bromide machine, the desorber heat should be supplied at a temperature of approximately 90°C.

When heat is applied to the solution in the desorber, the volatile component (water) is boiled off, and the vapor flows to the condenser. The remaining liquid solution exits the desorber and flows back to the absorber. The process in the desorber is a partial evaporation. As the vapor leaving the desorber is essentially free of salt, the liquid solution becomes concentrated during the partial evaporation process. Thus, the solution flowing back to the absorber is a relatively concentrated salt solution (compared to that exiting the absorber).

The concentrated salt solution leaving the desorber passes through a solution heat exchanger, where it exchanges energy with the solution leaving the absorber. This heat exchange process occurs between two liquid streams and involves primarily sensible heat. The purpose of this internal heat exchange device is to reduce the external heat input requirement by utilising the energy available within the machine that would otherwise be wasted. By including a solution heat exchanger, the rate of rejected heat in the absorber is also reduced.

The solution stream leaving the desorber returns to the absorber. The stream gives up energy in the solution heat exchanger and typically arrives subcooled at the flow restrictor. As the liquid is throttled through the restrictor, some vapor may evolve from the liquid. The two-phase stream then enters the absorber. In the absorber, the concentrated salt solution is brought into contact with the vapor supplied by the evaporator. The absorption process occurs when an external sink, such as a flow from a cooling tower cools the absorber. As the vapor is absorbed, the liquid mass fraction is reduced to the level of the desorber input.

The refrigerant leg takes the refrigerant vapor from the desorber and directs it to the condenser, where it is liquefied by rejecting heat to a sink. In a typical installation, the absorber and the condenser would reject heat to the same sink. The subcooled liquid leaving the condenser is throttled through the restrictor to the low pressure. This throttling process is typically accompanied by some vapor flashing. The two-phase refrigerant then enters the evaporator. Evaporation takes place, accompanied by heat transfer from the evaporator environment to the

evaporator, due to the low pressure created by the absorber. Complete evaporation then implies that all the refrigerant flow arrives at the absorber as vapor.

The typical pressures in a single-effect LiBr absorption machine are subatmospheric. The vapour pressure characteristics of the refrigerant in the working fluid mixtures determine the values of the pressures in the cycle. As essentially pure water exists in the condenser and evaporator, the temperature of operation of these components defines the high and low pressures. The lowest pressure in an absorption machine is in the evaporator and absorber, with typical pressures on the order of 1 kPa for space cooling applications.

The nature of salt solutions, such as aqueous LiBr, is that the salt component precipitates when the mass fraction of salt exceeds the solubility limit. The solubility limit is a strong function of mass fraction and temperature, and a weak function of pressure. The phenomenon of precipitation of salt from an aqueous solution can be readily observed by preparing a solution of 0.70 mass fraction LiBr. The two-phase regions adjacent to the liquid region consist of solid hydrate along with liquid solution. This is typical of the wet solid that can form in the absorption machine piping if machine conditions wander from design conditions. The solid precipitate tends to cling to piping components, and if conditions persist, it can entirely clog the flowing system, stopping the flow. Water-cooled absorption machines can generally operate year-round without crystallisation problems if they are well-maintained and carefully monitored [8] .

3.2. The Commercial Absorption Chiller

The commercial absorption chiller used in the Córdoba demo site is a single-effect hot water-fired LiBr/water absorption chiller supplied by Carrier. This absorption machine is the model 16LJ-F14E-LC with serial number MC0156, and a cooling capacity of 413 kW under nominal conditions. Figure 3.2 illustrates the refrigeration cycle of this chiller, with the legend corresponding to its components [7] .

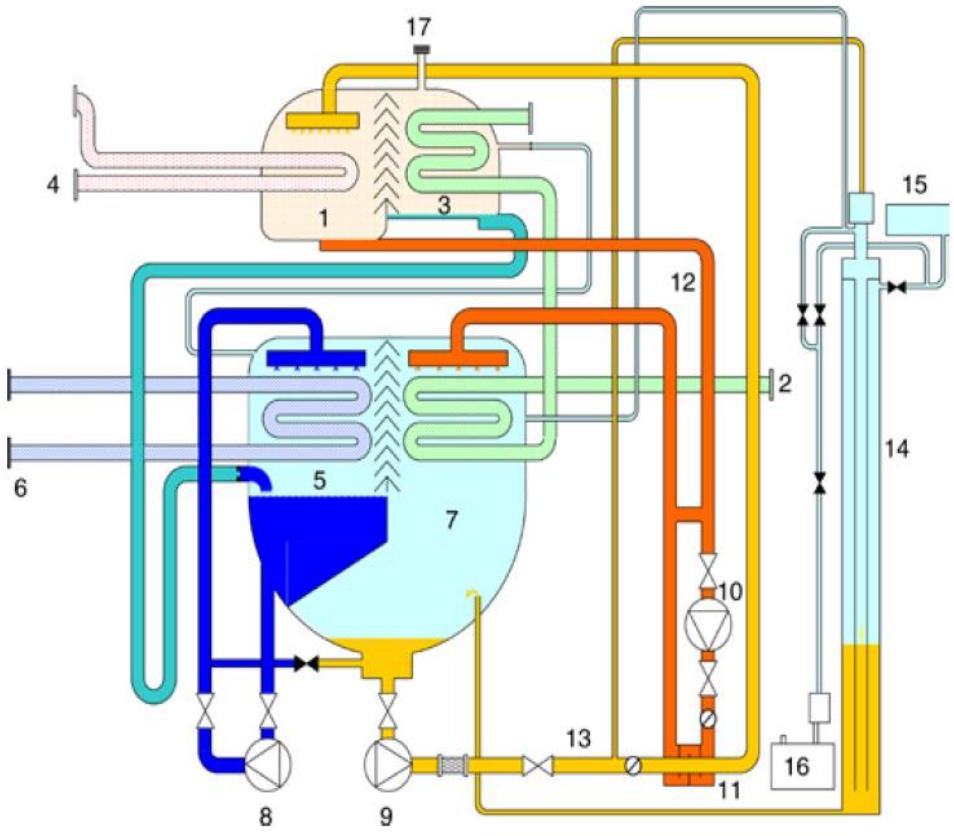

1. Generator
2. Cooling water
3. Condenser
4. Hot water
5. Evaporator
6. Chilled water
7. Absorber
8. Refrigerant pump
9. Absorbent pump 1
10. Absorbent pump 2
11. Solution heat exchanger
12. Concentrated solution
13. Diluted solution
14. Purge unit
15. Purge tank
16. Purge pump
17. Rupture disk

Figure 3.2. Carrier model 16LJ-F14E-LC absorption chiller.

The Carrier absorption chiller has the configuration shown in the image above. This chiller consists of two cylindrical shells, each housing two components that operate at approximately the same pressure. The evaporator and absorber are in the shell where the pressure is lower, and the generator and condenser are in the other shell where the pressure is higher. These pressures are subatmospheric.

The refrigerant, which leaves the condenser, is dispersed on the heat transfer tubes of the evaporator after passing through the refrigerant pump. The chilled water through the tubes is cooled by the latent heat of the vaporised refrigerant. The concentrated solution coming from the heat exchanger is dispersed on the heat transfer pipes of the absorber. The concentrated solution absorbs the refrigerant vapor from the evaporator. The diluted solution, after leaving the absorber section, passes through the pump and the heat exchanger, where it is heated by the concentrated solution leaving the generator. Consequently, the concentrated solution is cooled by the diluted solution, which increases the concentrated solution's absorption capability due to its lower temperature. The diluted solution from the heat exchanger is heated in the generator, where the heat from the hot water separates the refrigerant vapour, which is directed

to the condenser, and the concentrated solution, which is returned to the absorber. The cooling water that passes across the external tubes from the condenser inlet to the absorber outlet is heated by the condensation heat and the absorption heat. Regarding the purge unit, the non-condensable gas inside the chiller is stored in the purge tank. The chiller features a rupture disc at the top of the generator to protect the equipment in the event of overpressure [9] .

3.2.1. Chiller Sensors

The system includes a control centre, power supply, temperature and pressure sensors, and all necessary auxiliary devices required for safe and proper operation of the chiller. Next, Figure 3.3 shows a flow diagram of the chiller with its respective sensors, which are identified in Table 3.1 [10] .

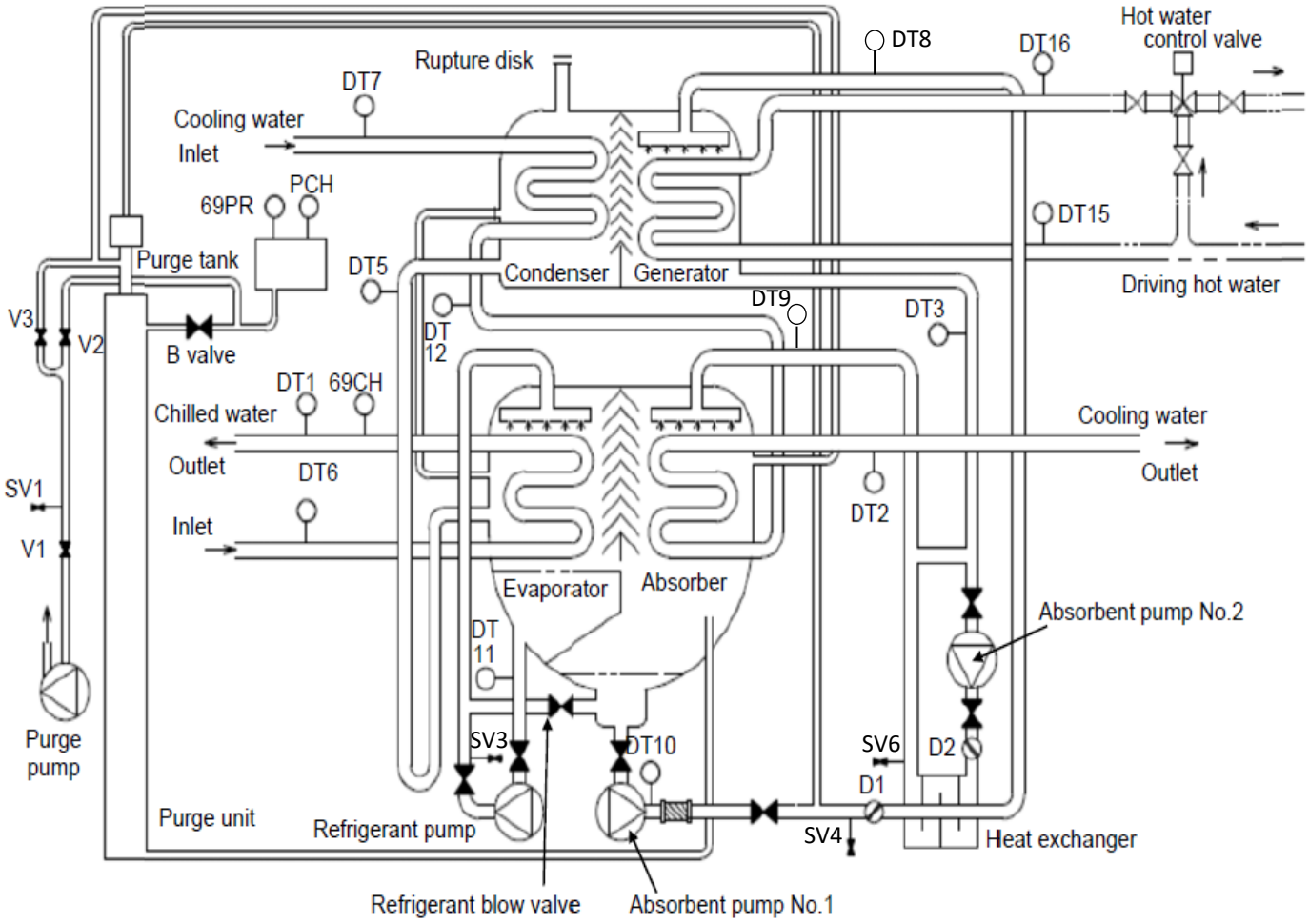

Figure 3.3. Carrier absorption chiller flow diagram.

Table 3.1. List of Carrier absorption chiller sensors.

Symbol	Name
DT1	Chilled water outlet temperature
DT2	Cooling water outlet temperature
DT3	Generator outlet solution temperature
DT5	Condenser outlet temperature
DT6	Chilled water inlet temperature
DT7	Cooling water outlet temperature
DT8	Generator inlet temperature
DT9	Absorber inlet solution temperature
DT10	Absorber outlet temperature
DT11	Evaporator inlet temperature
DT12	Cooling water mid temperature
DT15	Hot water inlet temperature
DT16	Hot water outlet temperature
69CH	Chilled water flow switch
PCH	Palladium cell heater
69PR	Purge tank pressure

Apart from the sensors, some device symbols are not mentioned in the diagram. D1 and D2 are the diluted solution main damper and the refrigerant damper, respectively, and they have the function of reducing or eliminating unwanted vibrations and movements in these streams. The SV symbol corresponds to service valves, which function to isolate parts of the system, allowing tasks such as connecting pressure gauges, charging or discharging refrigerant, or performing a vacuum, without interrupting the overall system operation. SV1 is the charge or discharge N_2 gas service valve, SV3 is the refrigerant service valve, SV4 is the diluted solution service valve, and SV6 is the concentrated solution service valve. Finally, V1, V2 and V3 correspond to manual purge valves.

3.2.2 Carrier Control System

The Carrier control system is a digital PID (proportional plus integral plus derivative) control that maximises unit performance by maintaining a ±0.5 K variance in leaving chilled-water temperature from the setpoint. The controller's innovative design also incorporates the ability to start and stop the system's chilled and hot water pumps, as well as stabilising the chilled and hot water temperature with high accuracy.

At startup, the opening angle of the hot-water control valve is controlled in three stages, reducing the amount of hot water and the time required to reach the desired level. The hot water control valve is positioned by the PID control algorithm to ensure precise control of the desired chilled water temperature without overshooting the set point [7] .

4- PERFORMANCE OF THE ABSORPTION CHILLER

In this section, the performance of the absorption chiller is calculated at both nominal conditions and commissioning proof conditions.

4.1 Performance of the Absorption Chiller at Nominal Conditions

As mentioned earlier, the primary objective of this master's thesis is to investigate the performance of the Carrier absorption chiller, model 16LJ-F14E-LC. It is a single-effect hot water-fired absorption chiller that uses LiBr/water as the working fluid mixture. Table 4.1 shows the chiller specifications provided by Carrier at nominal conditions.

Table 4.1. Carrier model 16LJ-F14E-LC absorption chiller specifications.

Model name:	16LJ-F14E-LC		
Cooling capacity		413	kW
Chilled water	Inlet temperature	12.0	ºC
	Outlet temperature	6.0	ºC
	Flow rate	59.2	m^3/h
	Pressure drop	61.9	kPa
	Max. working pressure	1034	kPa
Cooling water	Inlet temperature	30.0	ºC
	Outlet temperature	35.0	ºC
	Flow rate	163	m^3/h
	Pressure drop	68.8	kPa
	Max. working pressure	1034	kPa
Hot water	Inlet temperature	95.0	ºC
	Outlet temperature	76.2	ºC
	Flow rate	25.2	m^3/h
	Pressure drop	95.0	kPa
	Max. working pressure	1034	kPa
Electric motor output	No.1 absorbent pump	1.5	kW

No.2 absorbent pump	0.2	kW
Refrigerant pump	0.2	kW
Purge pump	0.4	kW

Using the specification data, the driving hot water and cooling water heat rates, as well as the thermal COP and other energy efficiency indicators, can be calculated under nominal conditions. The thermal coefficient of performance (COP_{th}) is a performance indicator that is defined as the ratio of cooling capacity to the driving heat rate supplied to the generator for activation. The higher the COP, the more efficient the machine is.

The thermal load of the generator, which is the same as the hot water heat rate, is calculated by using the following equation 4.1:

$$\dot{Q}_G = \frac{\dot{V}_{hw}}{3600} \cdot \rho_{hw} \cdot Cp_{hw}(T_{hw,in} - T_{hw,out}) \tag{4.1}$$

where $\dot{V}_{hw}$ is the volumetric flow rate of the hot water circuit in m^3/h, ρ_{hw} is the density in kg/m^3 and Cp_{hw} is the specific heat of water in kJ/kg·ºC. The last two properties are calculated at the mean value of the inlet and outlet temperatures of hot water $T_{hw,in}$ and $T_{hw,out}$.

The result of the thermal load of the generator is 535.3 kW. Now, with the cooling capacity having a value of 413 kW, the thermal COP can be calculated as:

$$COP_{th} = \frac{\dot{Q}_E}{\dot{Q}_G} = 0.772 \tag{4.2}$$

Another energy efficiency indicator used to evaluate the performance of the absorption chiller is the exergy COP. The ECOP is calculated with the equation shown below.

$$ECOP = \frac{|\dot{Q}_E \cdot (1 - \frac{T_0}{T_E})|}{\dot{Q}_G \cdot \left(1 - \frac{T_0}{T_G}\right) + W} \tag{4.3}$$

where T_0 is the reference ambient temperature, taken as 298 K, T_E is the average value of the inlet and outlet temperatures of chilled water in K, and T_G is the average value of the inlet and outlet temperatures of hot water in Kelvin. W is the total power of the solution, refrigerant and purge pumps, taken as 2.3 kW. The result of the ECOP is 0.253.

Finally, the specifications data can also be used to calculate the heat rate of the cooling water, which corresponds to the sum of the cooling heat rates of the absorber and the condenser.

$$\dot{Q}_{CA} = \frac{\dot{V}_{cw}}{3600} \cdot \rho_{cw} \cdot Cp_{cw}(T_{cw,out} - T_{cw,in}) \tag{4.4}$$

where $\dot{V}_{cw}$ is the volumetric flow rate of the cooling water circuit in m^3/h, ρ_{cw} is the density in kg/m^3 and Cp_{cw} is the specific heat of water in kJ/kg·ºC. The last two thermodynamic properties are calculated at the average value of the inlet and outlet temperatures of the cooling water, $T_{cw,in}$ and $T_{cw,out}$. The result is 941.3 kW.

The difference between the energy rate input and output is: 950.6 kW-941.3 kW=9.3 kW, around 1% of the heat rate input.

4.2. Performance of the Absorption Chiller at the Commissioning Proof Conditions

The Carrier absorption chiller model 16LJ-F14E-LC, with serial number MC0156, was commissioned on October 2, 2024. The chiller was in operation for 3 hours. The set data provided by Carrier corresponds to the temperature values of the internal and external streams. The cooling capacity and the driven hot water heat rate were measured by the University of Cordoba.

4.2.1. Commissioning Proof Experimental Data

The input data used for calculating performance at the commissioning proof conditions are the data provided by Carrier, corresponding to the different temperatures of the sensors described in Section 3.2.1. Chiller Sensors) and the flow rate of chilled water circulating in the external circuit of the evaporator is supplied by the Cordoba University.

The values of the identified input data are shown below:

- Generator data:
  - T_{15} = 84.1 ºC (hot water inlet temperature)
  - T_{16} = 65.5 ºC (hot water outlet temperature)
  - T_3 = 67.0 ºC (outlet concentrated solution temperature)
  - T_8 = 58.3 ºC (inlet diluted solution temperature)

- Evaporator data:
  - T_6 = 13.8 ºC (chilled water inlet temperature)
  - T_1 = 8.5 ºC (chilled water outlet temperature)
  - T_{11} = 7.2 ºC (saturated refrigerant temperature)
  - $\dot{V}_{chw}$ = 64.1 m^3/h (chilled water volumetric flow rate)
- Condenser/Absorber data:
  - T_7 = 26.0 ºC (cooling water inlet temperature at condenser)
  - T_{12} = 29.1 ºC (cooling water mid temperature)
  - T_2 = 31.6 ºC (cooling water outlet temperature at absorber)
  - T_5 = 29.5 ºC (outlet refrigerant temperature at condenser)
  - T_{10} = 31.5 ºC (outlet diluted solution temperature at absorber)
  - T_9 = 35.0 ºC (inlet concentrated solution temperature at absorber)

It has been assigned uncertainties for the experimental data. For temperatures, an uncertainty value of ±0.5 °C is assumed. For the chilled water flow rate, an uncertainty of 1% of the flow rate value is applied, as this is a Sharky 775 ultrasonic flowmeter [11] . As the chilled water flow rate is 64.1 m^3/h, its uncertainty is ±0.64 m^3/h.

Apart from the temperatures identified in the chiller flow diagram, two additional temperatures are identified, which do not have a sensor and are therefore unknown variables. The first is the temperature of the refrigerant vapour flow leaving the generator to the condenser, which is referred to as T_4. The second is the evaporator outlet vapour refrigerant temperature going to the absorber, which is named T_{13}.

4.2.2. Modelling Assumptions

The following assumptions need to be made to model the chiller with the EES software:

- The system is working under steady-state conditions.
- Heat losses and pressure drops in heat exchangers and connecting pipes are neglected.
- The diluted solution at the absorber outlet is a saturated solution.
- The concentrated solution at the generator outlet (state 3) is a saturated solution.
- The stream that leaves the generator to the condenser (state 4) is pure water vapor.
- The vapor refrigerant at the generator outlet (state 4) is in equilibrium with the diluted solution at the generator inlet (state 8)
- The flow configuration of the generator is counter-current flow.

- The refrigerant at the condenser outlet (state 5) is saturated water liquid.
- The evaporation temperature is constant.
- The stream that leaves the evaporator to the absorber (state 13) is saturated water vapor.
- The electrical power of the pumps are not estimated.

4.2.3. Data Modelling

Once the input data and assumptions have been explained, it is possible to model the chiller using EES software. The equations and steps used to analyse the machine's performance are presented below. To carry out this modelling, the uncertainties of the data are determined with the EES program. The annexe shows the model of the EES carried out.

First, the pressures of the internal streams can be obtained. The highest pressure is obtained under the assumption that the refrigerant at the condenser outlet (state 5) is a saturated liquid. Therefore, the saturation pressure of the water at T_5 is calculated in the EES software. On the other hand, the lower pressure is obtained because the refrigerant at the evaporator outlet (state 13) is saturated water vapour, and the saturation pressure of water at T_{13} is calculated. From these pressures, all the pressures of the internal circuits can be determined, as it has been assumed that there are no pressure losses.

The mass fractions of the LiBr absorbent can also be calculated in the EES software. The composition of the concentrated solution is determined by the temperature of the outlet solution in the generator (state 3) and the pressure in the generator (higher pressure). On the other hand, the composition of the dilute solution is determined by the temperature of the outlet solution in the absorber (state 10) and the lower pressure. Although the T_{10} sensor is downstream of the absorbent pump 1 and is therefore at the highest pressure, it is worth noting that the low pressure was chosen for this calculation because the dilute solution at the equilibrium outlet of the absorber occurs at this pressure.

Once the pressures and mass fractions of LiBr are known, the missing temperature can be obtained. This temperature is T_4, which corresponds to the refrigerant leaving the generator on the way to the condenser. As it has been assumed that the generator has a counter-current flow, the T_4 is calculated from the LiBr mass fraction of stream 8 (dilute solution entering the generator) and from its pressure, which corresponds to the high pressure.

Now, the cooling capacity (evaporator heat duty) is calculated since the inlet and outlet temperatures of the chilled water and its volumetric flow rate are known.

$$\dot{Q}_E = \frac{\dot{V}_{chw}}{3600} \cdot \rho_{chw} \cdot Cp_{chw}(T_6 - T_1) \tag{4.5}$$

where $\dot{V}_{chw}$ is the volumetric flow rate of the chilled water circuit in m^3/h, ρ_{chw} is the density in kg/m^3 and Cp_{chw} is the specific heat of water in kJ/kg ºC. The last two parameters are calculated with the EES software based on the average value of the inlet and outlet temperatures of chilled water, T_6 and T_1. The result of the cooling capacity is 395.6 kW with an uncertainty of ± 52.9 kW.

The next step is to calculate the heat rates of the remaining equipment. For this, the internal flow rates and their enthalpies must be known. The enthalpies can be calculated with the EES software, since for the solution streams the temperature and the mass fraction of LiBr is known, and for the water streams the temperature and the pressure or saturation state is known.

First, the refrigerant flow rate is calculated from the energy balance in the evaporator.

$$m_5 = \frac{\dot{Q}_E}{(h_{13} - h_5)} \tag{4.6}$$

where $\dot{Q}_E$ is the cooling capacity calculated previously in kW, h_{13} and h_5 are the enthalpies in these states in kJ/kg, and m_5 is the refrigerant flow rate in kg/s .The flow rate in state 5 is the same as streams in states 4,11 and 13, because the flow in these states is the refrigerant.

After calculating the refrigerant flow rate, the dilute solution flow rate and the concentrated solution flow rate can be calculated. To calculate these flow rates, an overall mass balance (4.7) and a LiBr mass balance (4.8) are applied in the generator.

$$m_8 = m_3 + m_4 \tag{4.7}$$

$$m_8 \cdot x_8 = m_3 \cdot x_3 \tag{4.8}$$

where m_8 is the diluted solution flow rate and m_3 is the concentrated solution flow rate. The flow rate in state 8 is the same as state 10 and the flow rate in state 3 is the same as state 9. The symbol x corresponds to the LiBr mass fraction.

The thermodynamic properties and flow rates of the internal streams are shown in Table 4.2 below.

Table 4.2. Thermodynamic properties and flow rates of the internal streams

State point	T (ºC)	P (kPa)	m (kg/s)	h (kJ/kg)	x (LiBr mass fraction)
3	67.0	4.127	1.657	156.9	0.572
4	56.7	4.127	0.166	2606	0
5	29.5	4.127	0.166	123.6	0
8	58.3	4.127	1.823	125.4	0.520
9	35.0	1.016	1.657	93.42	0.571
10	31.5	4.127	1.823	68.38	0.520
11	7.2	1.016	0.166	30.27	0
13	7.2	1.016	0.166	2514	0

Since the internal flow rates have been calculated, the solution circulation ratio can now be calculated. This term is the ratio of the mass flow rate of the inlet solution to the outlet refrigerant mass flow rate in the generator.

$$f = \frac{m_8}{m_4} \tag{4.9}$$

The solution circulation ratio is 11.01, i.e., the inlet solution flow rate is 11 times higher than the outlet refrigerant flow rate.

The heat duty in the condenser can then be calculated by doing the energy balance because the refrigerant flow rate is now known.

$$\dot{Q}_C = m_4 \cdot (h_4 - h_5) \tag{4.10}$$

The result of the condenser heat rate is 410.8 kW $\pm$ 55.0 kW.

As before, the enthalpies and mass flow rates of the internal streams have been calculated, the driving energy in the generator is calculated by using the following energy balance equation.

$$\dot{Q}_G = m_3 \cdot h_3 + m_4 \cdot h_4 - m_8 \cdot h_8 \tag{4.11}$$

The generator driving heat energy is 462.8 kW with an uncertainty of ± 62.1 kW

Finally, the heat duty of the absorber is calculated. As in the case of the generator, all the variables are known to calculate it. The energy balance equation for the absorber is shown below.

$$\dot{Q}_A = m_9 \cdot h_9 + m_{13} \cdot h_{13} - m_{10} \cdot h_{10} \quad (4.12)$$

The absorber heat duty is 446.2 kW $\pm$ 59.7 kW.

The difference between the energy input and output in the absorption chiller can be written as

$$DIF_E = Q_E + Q_G - Q_C - Q_A \quad (4.13)$$

This term has a value of 1.3 kW $\pm$ 4.3 kW. Considering that the electrical powers of the pump have been neglected and are usually around 1 kW, it can be concluded that the heat losses are negligible.

Once the thermal loads of the main components of the absorption chiller (generator, absorber, evaporator and condenser) have been calculated, the heat duty of the solution heat exchanger and its efficiency can also be calculated. The equations for calculating these are shown below.

$$\dot{Q}_{SHX} = m_{10} \cdot (h_8 - h_{10}) \quad (4.14)$$

$$eff_{SHX} = \frac{T_3 - T_9}{T_3 - T_{10}} \quad (4.15)$$

The solution heat exchanger heat duty is 103.9 kW $\pm$ 17.0 kW and its effectiveness is 90.1% $\pm$ 1.9%. This efficiency is high, because the heat exchanger is a plate heat exchanger.

Two different indicators are used to evaluate the performance of the absorption chiller: thermal coefficient of performance (COP_{th}) and exergy coefficient of performance (ECOP). As discussed above, thermal COP assesses thermal performance as ratio of cooling capacity to heat supplied to the generator for activation:

$$COP_{th} = \frac{\dot{Q}_E}{\dot{Q}_G} \quad (4.16)$$

The thermal COP has a value of 0.855 with an uncertainty of ± 0.009.

The exergy coefficient of performance is calculated from the following equation:

$$ECOP = \frac{|\dot{Q}_E \cdot (1 - \frac{T_0}{T_E})|}{\dot{Q}_G \cdot (1 - \frac{T_0}{T_G})} \quad (4.17)$$

Where T_0 is the ambient temperature in K (it is supposed 298 K), T_E is the average value of the inlet and outlet temperatures of chilled water in K, and T_G is the average value of the inlet and outlet temperatures of hot water in K. The result of the ECOP is 0.291 with an uncertainty of ± 0.009.

After the performance indicators have been calculated, the external flow rates of hot water and cooling water are also calculated.

First, the energy balance in the generator allows to calculate the flow rate of the hot water stream

$$\dot{V}_{hw} = \frac{\dot{Q}_G}{\rho_{hw} \cdot Cp_{hw}(T_{15} - T_{16})} \cdot 3600 \quad (4.18)$$

where $\dot{Q}_G$ is the generator heat rate in kW, ρ_{hw} is the density in kg/m^3 and Cp_{hw} is the specific heat of water in kJ/kg·ºC. The last two parameters are calculated with the EES software based on the average value of the inlet and outlet temperatures of hot water, T_{15} and T_{16}. The result of the hot water flow rate is 21.9 m^3/h with an uncertainty of ± 3.1 m^3/h.

The University of Cordoba has provided the hot water flow rate as it was measured with a flow meter. The value of this flow rate is 23.3 m^3/h, so it is within the range of the calculated value of hot water with the model.

Now, the energy balance in the absorber and condenser is stated to estimate the cooling water heat rate. In this case, it is essential to consider that the cooling flow connects the condenser and the absorber.

$$\dot{V}_{cw} = \frac{\dot{Q}_C + \dot{Q}_A}{\rho_{cw} \cdot Cp_{cw}(T_2 - T_7)} \cdot 3600 \quad (4.19)$$

where $\dot{Q}_C$ is the condenser heat rate in kW, $\dot{Q}_A$ is the absorber heat rate in kW, ρ_{cw} is the density in kg/m^3 and Cp_{cw} is the specific heat of water in kJ/kg·ºC. The last two parameters are

calculated with the EES software based on the average value of the inlet and outlet temperatures of cooling water, T_2 and T_7. The result of the cooling water flow rate is 132 m^3/h with an uncertainty of ± 24 m^3/h.

Finally, the model is used to calculate the UA values for the thermal components of the chiller. Thus, the product of the overall heat transfer coefficient, U, and the heat exchanger area, A, is a convenient way to specify the size and performance of a heat exchanger in a single parameter. To obtain this product, the logarithmic mean temperature differences of the different heat exchangers are first calculated.

$$\Delta_E = \frac{T_6 - T_{13} - (T_1 - T_{11})}{\ln \frac{T_6 - T_{13}}{T_1 - T_{11}}} = 3.26 \pm 0.70 \text{ K} \tag{4.20}$$

$$\Delta_A = \frac{T_{10} - T_{12} - (T_9 - T_2)}{\ln \frac{T_{10} - T_{12}}{T_9 - T_2}} = 2.87 \pm 0.51 \text{ K} \tag{4.21}$$

$$\Delta_C = \frac{T_5 - T_7 - (T_4 - T_{12})}{\ln \frac{T_5 - T_7}{T_4 - T_{12}}} = 11.68 \pm 0.96 \text{ K} \tag{4.22}$$

$$\Delta_G = \frac{T_{16} - T_4 - (T_{15} - T_3)}{\ln \frac{T_{16} - T_4}{T_{15} - T_3}} = 12.47 \pm 0.75 \text{ K} \tag{4.23}$$

$$\Delta_{shx} = \frac{T_3 - T_8 - (T_9 - T_{10})}{\ln \frac{T_3 - T_8}{T_9 - T_{10}}} = 5.71 \pm 0.56 \text{ K} \tag{4.24}$$

Now, it is possible to calculate the overall heat transfer coefficient-area product (UA). Next, it is shown the heat exchangers equations.

$$UA_E = \frac{\dot{Q}_E}{\Delta_E} = 121 \pm 35 \text{ kW/K} \tag{4.25}$$

$$UA_A = \frac{\dot{Q}_A}{\Delta_A} = 155 \pm 34 \text{ kW/K} \tag{4.26}$$

$$\mathrm{UA_C} = \frac{\dot{\mathrm{Q}}_\mathrm{C}}{\Delta_\mathrm{C}} = 35.2 \pm 5.5\ \mathrm{kW/K} \tag{4.27}$$

$$\mathrm{UA_G} = \frac{\dot{\mathrm{Q}}_\mathrm{G}}{\Delta_\mathrm{G}} = 37.1 \pm 5.6\ \mathrm{kW/K} \tag{4.28}$$

$$\mathrm{UA_{shx}} = \frac{\dot{\mathrm{Q}}_\mathrm{shx}}{\Delta_\mathrm{shx}} = 18.2 \pm 3.8\ \mathrm{kW/K} \tag{4.29}$$

Knowing the external flow rates of hot, cooling, and chilled water, as well as the temperatures of the hot water inlet, cooling water inlet, and chilled water outlet, the UAs model is able to determine the operation of the absorption chiller.

5- Conclusions

In this master's thesis, the results of commissioning the Carrier absorption chiller have been used to model and evaluate its performance, including heat exchange rates in the main thermal components, as well as the thermal and exergy COP performance indicators.

The model used is considered valid, as discussed in the results, since the value of the external hot water flow rate provided by the University of Córdoba falls within the range of the hot water value calculated using the model.

Additionally, the overall heat transfer coefficient-area product (UA) allows for the determination of internal variables and the chiller's performance.

In summary, the model is effective and can be used to determine performance and behaviour under various operating conditions.

6- References

[1] WEDISTRICT. (n.d.). *About WEDISTRICT*. Accessed: February 27 2025. https://www.wedistrict.eu/project/#about

[2] European Union. (2024, November 12). *Smart and local renewable energy DISTRICT heating and cooling solutions for sustainable living (WEDISTRICT) [Project ID 857801]*. CORDIS. Accessed: March 1 2025. https://cordis.europa.eu/project/id/857801

[3] European Union. (2024). *Results of new DHCs demonstration – Alcalá demo* [Deliverable]. In *Smart and local reneWable Energy DISTRICT heating and cooling solutions for sustainable living (WEDISTRICT, Grant No. 857801)*. CORDIS. Accessed: March 7 2025. https://cordis.europa.eu/project/id/857801/results

[4] WEDISTRICT. (n.d.). *Córdoba demonstration case*. Accessed: March 10 2025. https://www.wedistrict.eu/demonstration-cases/cordoba/

[5] WEDISTRICT. (2023). *Deliverable D8.3: Demonstration of district heating and cooling systems*. Accessed: March 20 2025. https://www.wedistrict.eu/wp-content/uploads/2023/09/Deliverable_D8.3_DHC_Systems.pdf

[6] CONAMA. (2020). *Results and challenges of renewable energy integration in district heating and cooling systems* [PDF]. *CONAMA 2020*. Accessed: March 23 2025. http://www.conama11.vsf.es/conama10/download/files/conama2020/CT%202020/5428.pdf

[7] Carrier. (n.d.). *16LJ/LJF: Energy-efficient solutions for heating and cooling systems*. Accessed: April 1 2025. https://ahi-carrier.gr/wp-content/uploads/16LJ_LJF.pdf

[8] Herold, K. E., Radermacher, R., & Klein, S. A. (2016). Absorption Chillers and Heat Pumps (2nd ed.). CRC Press. Accessed: April 8 2025.

[9] Panasonic Corporation. (n.d.). Specifications: Absorption Chiller Model 16LJ-F14E-LC (Spec No. 2- MC0156-00). Panasonic Corporation. Accessed: April 20 2025.

[10] Carrier. (n.d.). OPERATION MANUAL: Absorption Chiller 16LJ-F Series (ACQA36-00270). CARRIER SCS. Accessed: April 30 2025.

[11] Diehl Metering. (n.d.). *SHARKY 775 FR*. Accessed: June 10 2025. https://www.diehl.com/metering/es/productos-y-soluciones/productos-servicios/medicion-de-energia-termica/sharky-775-fr/

A- ANNEX

A.1. EES Model

```
"Carrier LiBr/Water absorption chiller"

"Generator"
T[15]=84,1 [C] "hot water inlet temperature"
T[16]=65,5 [C] "hot water outlet temperature"
T[3]=67,0 [C] "outlet concentrated solution temperature"
T[8]=58,3 [C] "inlet diluted solution temperature"
"State 4 is outlet refrigerant temperature"

"Evaporator"
T[6]=13,8 [C] "chilled water inlet temperature"
T[1]=8,5 [C] "chilled water outlet temperature"
T[11]=7,2 [C] "inlet refrigerant temperature"
Q[11]=0 "state 11 is saturated water liquid at P_low"
"State 13 is outlet refrigerant temperature"

"Condenser/Absorber"
T[7]=26,0 [C] "cooling water inlet temperature at condenser"
T[12]=29,1 [C] "cooling water mid temperature"
T[2]=31,6 [C] "cooling water oulet temperature at absorber"
T[5]=29,5 [C] "outlet refrigerant temperature at condenser"
T[10]=31,5 [C] "outlet diluted solution temperature at absorber"
T[9]=35,0 [C] "inlet concentrated solution temperature at absorber"

"Chilled water volumetric flow rate"
V_chw=64,1 [m3/h]
V[6]=V_chw/3600 [m3/s]
V[1]=V[6]

"Chilled water properties"
T_mchw=(T[1]+T[6])/2 "chilled water mean temperature "
cp_chw=cp(Water;T=T_mchw;x=0)
rho_chw=density(Water;T=T_mchw;x=0)
m[6]=V[6]*rho_chw
m[1]=m[6]

"Evaporator heat rate (cooling capacity)"
Q_E=V[6]*rho_chw*cp_chw*(T[6]-T[1])

"Assumptions"
"State 10 is saturated solution"
"State 3 is saturated solution"
"State 4 is vapor state at equilibrium with the solution for x[8] and P_high; it is assumed that this vapor
is pure water"
"It is assumed that the flow configuration of the desorber is counter-current flow, so
T[4]=T(x[8],P_high)"
Q[5]=0 "State 5 is saturated water liquid at P_high"
T[13]=7,2 [C] "it is assumed that the evaporation temperature is the same in the inlet and outlet"
Q[13]=1 "State 13 is saturated water vapor at P_low"

"Pressures"
P_high=p_sat(Water;T=T[5])
P_low=p_sat(Water;T=T[11])
P[8]=P_high
P[3]=P_high
```

```
P[4]=P_high
P[5]=P_high
P[11]=P_low
P[13]=P_low
P[10]=P_high
P[9]=P_low

"LiBr mass fraction"
x[10]=x_librh2o(T[10];P_low) "the pressure to calculate it is P_low because the absorber outlet solution occurs in this pressure, and the temperature sensor T10 is after the absorbent pump 1"
x[3]=x_librh2o(T[3];P_high)
x[8]=x[10]
x[9]=x[3]
x[4]=0
x[5]=0
x[11]=0
x[13]=0

"Temperature 4"
T[4]=t_librh2o(P_high;x[8])

"Enthalpies"
h[8]=h_librh2o(T[8];x[8])
h[3]=h_librh2o(T[3];x[3])
h[4]=enthalpy(Water;T=T[4];P=P[4])
h[5]=enthalpy(Water;T=T[5];x=Q[5])
h[11]=enthalpy(Water;T=T[11];x=Q[11])
h[13]=enthalpy(Water;T=T[13];x=Q[13])
h[10]=h_librh2o(T[10];x[10])
h[9]=h_librh2o(T[9];x[9])

"Overall mass balance"
m[8]=m[3]+m[4]

"LiBr mass balance"
m[8]*x[8]=m[3]*x[3]

"Solution circulation ratio"
f=m[8]/m[4]

"Mass balances"
m[10]=m[8]
m[9]=m[3]
m[5]=m[4]
m[11]=m[4]
m[13]=m[4]

"Energy balance Evaporator"
Q_E=m[5]*(h[13]-h[5])

"Energy balance Condenser"
Q_C=m[4]*(h[4]-h[5])

"Energy balance Solution Heat Exchanger"
eff_shx=(T[3]-T[9])/(T[3]-T[10])
Q_shx=m[10]*(h[8]-h[10])

"Energy balance Generator"
Q_G=m[3]*h[3]+m[4]*h[4]-m[8]*h[8]
```

```
"Energy balance Absorber"
Q_A=m[9]*h[9]+m[13]*h[13]-m[10]*h[10]

"Thermal COP"
COP=Q_E/Q_G

"Exergy COP"
T_o=298 {K}
T_E=((T[6]+T[1])/2)+273
T_G=((T[15]+T[16])/2)+273
ECOP=abs(Q_E*(1-T_o/T_E))/(Q_G*(1-T_o/T_G))

"Error in Energy balance"
err_E=Q_E+Q_G-Q_C-Q_A

"Energy balance hot water (Generator)"
T_mhw=(T[15]+T[16])/2 "hot water mean temperature"
cp_hw=cp(Water;T=T_mhw;x=0)
rho_hw=density(Water;T=T_mhw;x=0)
m[16]=m[15]
Q_G=m[15]*cp_hw*(T[15]-T[16])
V[15]=m[15]/rho_hw
V[16]=V[15]
V_hw=V[15]*3600 [m3/h]

"Energy balance cooling water (Condenser+Absorber)"
T_mcw=(T[7]+T[2])/2 "cooling water mean temperature"
cp_cw=cp(Water;T=T_mcw;x=0)
rho_cw=density(Water;T=T_mcw;x=0)
m[2]=m[7]
m[12]=m[7]
Q_CA=Q_C+Q_A "cooling water heat rate"
Q_CA=m[7]*cp_cw*(T[2]-T[7])
V[7]=m[7]/rho_cw
V[2]=V[7]
V[12]=V[7]
V_cw=V[7]*3600 [m3/h]

"Logarithmic mean temperatures difference"
DTLM_E=((T[6]-T[13])-(T[1]-T[11]))/ln((T[6]-T[13])/(T[1]-T[11]))
DTLM_A=((T[10]-T[12])-(T[9]-T[2]))/ln((T[10]-T[12])/(T[9]-T[2]))
DTLM_C=((T[5]-T[7])-(T[4]-T[12]))/ln((T[5]-T[7])/(T[4]-T[12]))
DTLM_G=((T[16]-T[4])-(T[15]-T[3]))/ln((T[16]-T[4])/(T[15]-T[3]))
DTLM_shx=((T[3]-T[8])-(T[9]-T[10]))/ln((T[3]-T[8])/(T[9]-T[10]))

"Overall heat transfer coefficient-area product (UA)"
Q_E=UA_E*DTLM_E
Q_A=UA_A*DTLM_A
Q_C=UA_C*DTLM_C
Q_G=UA_D*DTLM_G
Q_shx=UA_shx*DTLM_shx
```

UNIVERSITAT
ROVIRA i VIRGILI